



HAL
open science

Low-energy cluster beam deposition : do you need it ?

P. Mélinon, G. Fuchs, B. Cabaud, A. Hoareau, P. Jensen, Vincent Paillard, M. Treilleux

► **To cite this version:**

P. Mélinon, G. Fuchs, B. Cabaud, A. Hoareau, P. Jensen, et al.. Low-energy cluster beam deposition : do you need it ?. Journal de Physique I, 1993, 3 (7), pp.1585-1603. 10.1051/jp1:1993202 . jpa-00246818

HAL Id: jpa-00246818

<https://hal.science/jpa-00246818>

Submitted on 4 Feb 2008

HAL is a multi-disciplinary open access archive for the deposit and dissemination of scientific research documents, whether they are published or not. The documents may come from teaching and research institutions in France or abroad, or from public or private research centers.

L'archive ouverte pluridisciplinaire **HAL**, est destinée au dépôt et à la diffusion de documents scientifiques de niveau recherche, publiés ou non, émanant des établissements d'enseignement et de recherche français ou étrangers, des laboratoires publics ou privés.

Classification
Physics Abstracts
61.16D — 81.15G

Low-energy cluster beam deposition : do you need it ?

P. Mélinon, G. Fuchs, B. Cabaud, A. Hoareau, P. Jensen, V. Paillard and M. Treilleux

Département de Physique des Matériaux (*). Université Claude Bernard-Lyon I. 43 Bd du 11 Novembre 1918, 69622 Villeurbanne Cedex, France

(Received 23 December 1992, accepted in final form 24 March 1993)

Abstract. — Physical and chemical properties of films prepared by Low-Energy Cluster Beam Deposition (LECBD) are presented, discussed and compared to those of films obtained by other conventional deposition techniques. LECBD films are formed by the stacking of individual grains corresponding roughly to the incident free clusters. This original structure suggests that LECBD is promising for technological and theoretical applications. Film properties strongly related to the mean grain size can be controlled with this original technique. This work shows several examples showing the assets of LECBD : ultrathin sintered films, high surface-volume ratio or continuous ultrathin films, new structures of metallic deposits. Used as a tool to obtain experimental data to study fractal 2D models or to elaborate deposits to study quantum size effects, this deposition technique would be original, efficient and sometimes essential in many research areas.

1. Introduction.

The interest in reproducible thin film growth has led to many recent advances in thin film deposition. Among the most recent techniques developed in this field, cluster beam deposition techniques present much interest. The first motivations to develop these original techniques were to produce either epitaxial films or supported size selected metal clusters that are structurally, physically and catalytically novel.

Because of the wide variety of source types found in the literature (Sattler-type, Smalley-type, Multiple Expansion Cluster Source (MECS), . . .) the ways to produce and deposit clusters appear to be numerous (Ionized Cluster Beam Deposition (ICBD), Reactive Cluster Beam Deposition (RCBD), Low-Energy Cluster Beam Deposition (LECBD), ...) [1]. The quenching of a molecular vapor inducing the formation of a cluster beam is the basic mechanism involved for all them. The diversity of these deposition techniques relies mainly first on the numerous ways to produce the molecular vapor or primary plasma (heated crucible, sputtering, laser ablation, . . .); to quench the molecular vapor in a cluster vapor (thermal cooling in a cold inert gas, adiabatic expansion through a nozzle, . . .) and to deposit clusters (with or without kinetic energy).

(*) Unité associée au CNRS.

Many studies have been published to illustrate the assets of film formation by using cluster beam. For instance, a spectacular example is the use of ICBBD for epitaxial film formation at room temperature between materials with large lattice mismatches [2-4]. Other examples are provided by the LECBD technique that allows the formation of ultrathin films [5] or metallic deposits presenting new structures [6-8].

The cluster beam characteristics (mean size of cluster distribution, kinetic energy, deposition rate, . . .) and the substrate temperature control the film growth and properties. As the real motivations of many studies are the new properties of the deposits, the characterization of the free cluster beam is neglected. In this way, the understanding of the basic phenomena responsible for the formation of the thin films from cluster beam is not achieved and the optimization of the chemical and physical properties is surely not reached. This is the reason why we think that particular attention has to be paid to characterize, when possible, the size distribution of the free cluster beam.

To know if the size distribution of free clusters plays a crucial role in the films elaborated by cluster beam deposition, many research programs are devoted to the selection and deposition of a given well-controlled size. However, to our knowledge, no film formation has been reported with selected size clusters. An intermediate stage is the use of a source giving a cluster beam with a narrow size distribution. The Sattler source-type [9] used for instance in the LECBD studies [10] presents a « clean » (without molecular vapor) and narrow size distribution. This source is considered as a first reasonable choice to conduct our systematic studies on the effect of cluster size on thin film formation and properties.

In this paper, we show that LECBD is a promising deposition technique for both technological and theoretical purposes because the grain size of the film is easily controlled. Using a Sattler source-type we compare the performance of this technique with molecular beam deposition (MBD). To minimize the interaction between the substrate and the deposited film, an amorphous substrate is selected. The physical and chemical thin LECBD film properties are presented from experimental results obtained on various elements (Bi, Sm, Sb). These examples enlighten the assets of LECBD : ultrathin sintered films, high surface-volume ratio or continuous ultrathin films, new structures of metallic deposits.

2. Experimental procedure.

The metallic vapor obtained from a heated crucible is used to perform MBD deposits or is cooled in an inert gas (He or Ar) at liquid nitrogen temperature to obtain a metallic cluster vapor. The cluster size, which is determined by the pressure and the nature of the gas, is measured by a time-of-flight mass-spectrometer before deposition. Figure 1a, b illustrates this point for Sb clusters. For low masses, previous results on fragmentation [11] lead us to believe that the ionized cluster mass distribution is a good measure of the neutral cluster size distribution. A wide range of incident cluster mean diameter has been explored and is given in table I. Although no mass selection is performed before deposition, the sharp width of the distribution (see typically Fig. 1b) is narrow enough to consider roughly a single cluster size (FWHM = 1 nm). The size distribution of low-energy clusters is also characterized by a total absence of molecular species (Sb₄). We have verified that the cluster beam is free of Sb₄. To avoid the problem of mass discrimination in the TOF apparatus, we have used the following experimental procedure. Without cold inert gas, the mass spectrometer is set up to observe the Sb₄⁺ signal (the electron energy used to ionize the beam is higher than the ionization potential (7.61 eV)). When the cold inert gas introduced, the Sb₄⁺ peak disappears and the signal of bigger clusters appears in the mass spectra. Size effects of the incident free clusters on the growth and properties of LECBD films are discussed now.

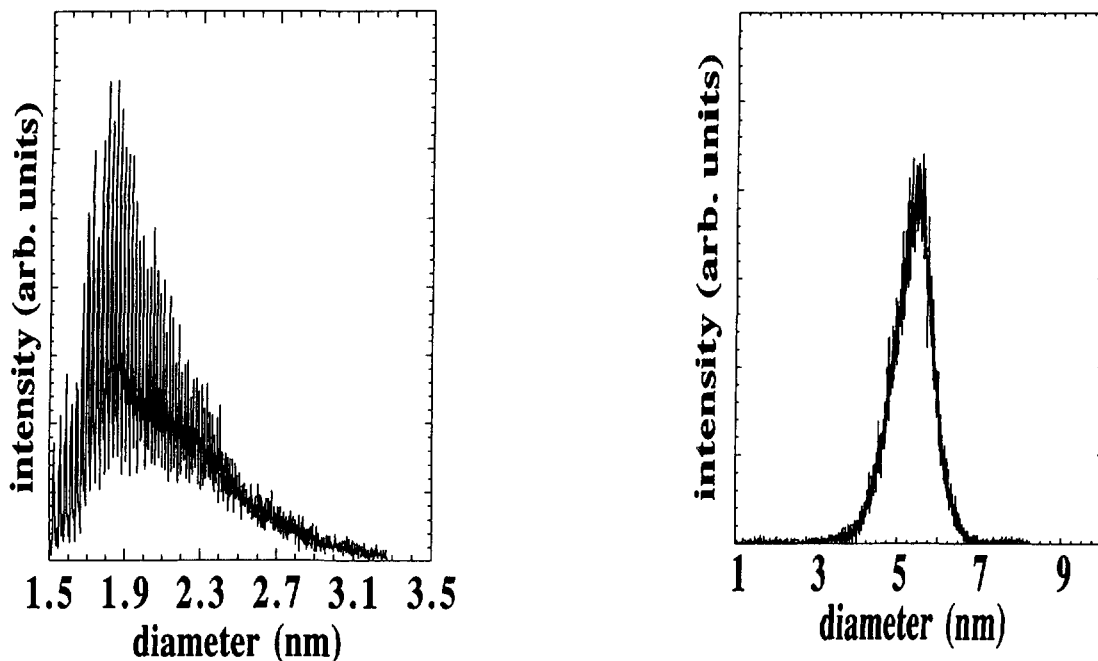


Fig. 1. — Size distribution of ionized antimony clusters assuming a spherical cluster shape and a density of bulk antimony. The size distribution is monitored by varying the pressure of the inert carrier gas. The cluster mean cluster size obtained with 100 Pa Ar pressure is 2 nm (a). Here each peak is the signature of the $(Sb_4)_N$ species and no complex $[(Sb_4)_x(O)_y]_N$ have been detected for large y ($y > 1$). The cluster mean size obtained with 10 Pa Ar pressure is 5 nm (b). Here, the $(Sb_4)_N$ species peaks cannot be resolved. In both cases (a, b), electron energy used to ionize Sb clusters is about 30 eV.

Table I. — Size range of free clusters used in our LECBD experiments : D_m is the cluster mean diameter and $\langle N \rangle$ the number of atoms per cluster.

Element	$\langle N \rangle$ (atoms)	D_m (nm)
In	1-100	0.4-1.7
Sb	4-2 500	0.6-5.2
Bi	2-1 100	0.5-4.3
Sm	400	0.4-2.9

To obtain a direct comparison between MBD and LECBD deposits, and so to study the first evidence of the free cluster size effect, films are synthesized in the same experimental system under the same deposition conditions (pressure, substrate temperature, deposition rate, ...). In both cases (MBD and LECBD deposition), the atomic or cluster vapor condenses on substrates maintained at room temperature. The residual vapor pressure is less than 10^{-4} Pa. During the evaporation, the deposited thickness d and the rate of deposition R are controlled by a crystal quartz monitor located near the substrate.

The deposits are characterized by *in situ* electrical measurements : since this method is very sensitive to impurities of the metal source, we underline that the very same source is used for MBD and LECBD deposits. After transfer through air, thin films are investigated by transmission electron microscopy (TEM), by Auger electron spectroscopy (AES), X-ray photoelectron spectroscopy (XPS) and Raman spectroscopy. Although further experimental details have been published previously [7, 12, 13], we would like to mention that the transfer through air may affect the real morphology of the deposits as they are in vacuum.

3. LECBD film growth.

In this section, we will focus on growth of *antimony* films to predict general properties of LECBD. Antimony films obtained by the conventional MBD technique have been extensively studied for their potential applications in electronic devices [14-16]. Our group was the first to grow antimony films by cluster deposition and to study the difference in the properties of the two kinds of films. The first and immediate difference in nucleation and growth process of MBD and LECBD deposits has been shown by TEM studies [17]. These observations show the high sensitivity of Sb deposits to the size of incident clusters. The increase of the size of incident clusters induces a decrease of the mean diameter D_m of the supported aggregates. This sensitivity is explained by the dependence of the sticking coefficient and the surface diffusion coefficient $D_{\langle N \rangle}$ versus $\langle N \rangle$ (where $\langle N \rangle$ is the cluster mean size) [13]. When the size of free low-energy clusters increases, their surface diffusion becomes low enough to neglect the growth of supported particles. Here, the size distribution of supported clusters roughly corresponds to that of free clusters. This is confirmed by TEM results obtained at low coverage with antimony clusters (mean size about 3.5 nm) deposited at room temperature (Fig. 2). The slight increase of the cluster size distribution between free and supported clusters (Fig. 2b) corresponds to a coalescence of about 5 incident clusters. This low coalescence regime is also confirmed by low temperature cluster deposition. When clusters are deposited at 150 K and covered in vacuum just after deposition (with a carbon fixing layer) the cluster size distribution is closer to the free cluster size distribution (in comparison with the 300 K-deposited clusters). Since in both cases (150 K and 300 K), the deposits have been protected by a fixing layer, the cluster surface diffusion cannot be modified by adsorption events between 150 K and 300 K. This experiment may be considered as an additional argument to show the low coalescence regime (compared to MBD). To specify the high coalescence regime during MBD growth, let us compare the morphology of 0.2 nm-thick deposits obtained by MBD and LECBD : MBD supported aggregates correspond to the coalescence of 5×10^4 incident Sb_4 while LECBD one correspond only to the coalescence of 5 incident particules. This low coalescence suggests that the growth of LECBD films can be compared to the filling of a random network in the percolation model. This powerful analogy [5] allows quantitative predictions of the electrical conduction threshold, coverage rate at the threshold, fractal dimension of the percolating path (called infinite cluster in the percolation model) and multifractal properties of the film. Electrical measurements and image analysis of TEM micrographs agree with the quantitative predictions [5, 18, 19].

This « paving » growth process occurs during the first stage of the film growth (less than a cluster-monolayer) and it is essential now to verify if it remains valid for higher thicknesses. TEM cross section of a 30 nm-thick film built from the stacking of 1 200 atom-clusters (Fig. 3) proves that film growth remains unchanged for higher thicknesses. The film morphology shows that the film grows from the random stacking of incident clusters. Besides, this TEM micrograph shows the low compactness of the film : the thickness measured from TEM is about 100 nm while RBS and crystal quartz measurements give a 30 nm-equivalent thickness. To obtain the film density profile from figure 3, the TEM image has been divided in columns

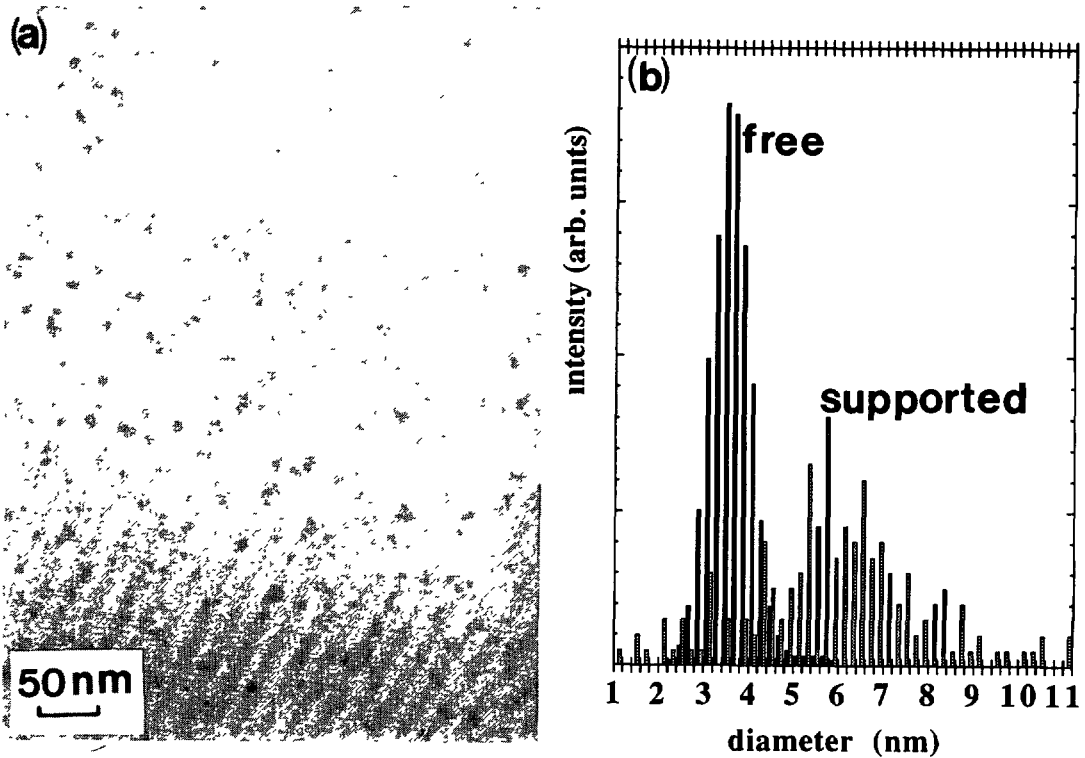


Fig. 2. — a) TEM micrograph of a 0.2 nm-thick antimony deposit obtained by LECBD at room temperature and 70 Pa Ar pressure ; b) the comparison between size distributions of free clusters (from time-of-flight mass spectra) and supported Sb clusters (from the TEM micrograph (a)) are presented. This indicates a low coalescence regime : the mean size of free and supported clusters is about 3.5 nm (800 atoms) and 6 nm respectively (4 000 atoms).

perpendicular to the interface. The width of each column corresponds to the mean size of the film grain diameter. Then we have counted the number of clusters n_c per column and reported the probability to fill one column with n_c clusters. So this histogram should be a narrow peak for a perfect smooth film. From the variation in cluster density presented in figure 4, the mean roughness R_{rms} has been calculated using the following formula :

$$R_{rms} = \left[\sum_i \frac{(Z_i - Z_m)^2}{N} \right]^{1/2}$$

where Z_i is the thickness of the film at the position i , Z_m the mean thickness, and N the total number of i positions. The value of $R_{rms} = 18$ nm found underlines the high roughness of the LECBD film. In the conventional continuous thin films (MBD for instance), the roughness corresponds only to a few Å.

4. Properties of LECBD deposits with controlled grain size.

Here, we refer to experiments for which the size of free clusters is large enough to produce a very low surface diffusion. So, the LECBD film grows from the random stacking of incident clusters and the average grain size of the film is about the same order of magnitude as the

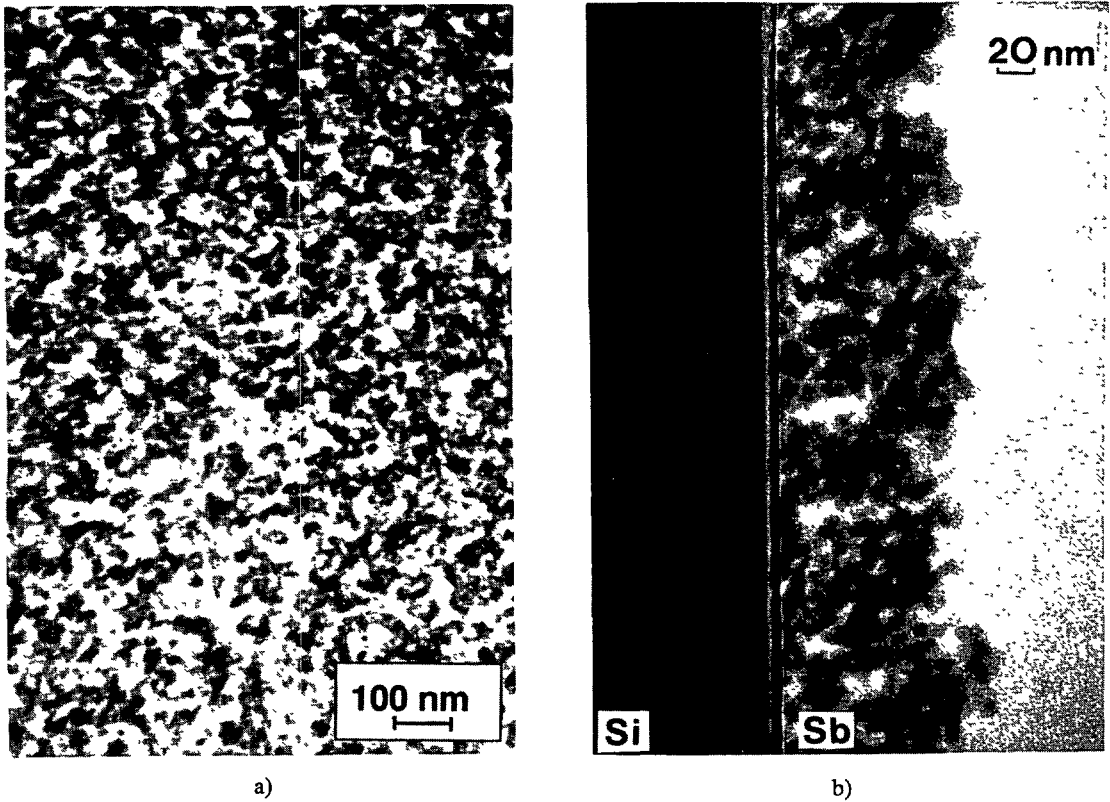


Fig. 3. — Plane view (a) and cross section (b) TEM images of LECBD Sb films. The mean grain size of the film is about 6 nm. This corresponds to the coalescence of about 4 incident free clusters.

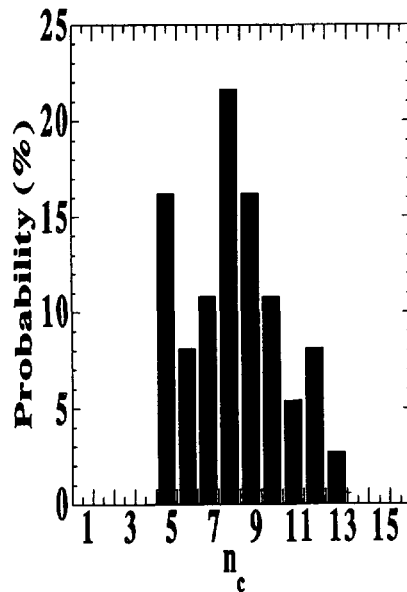


Fig. 4. — Roughness profile of the LECBD Sb film presented in figure 3b. The histogram presents the probability along the interface to fill a column with n_c clusters (see text).

incident free clusters. This original and unique (to our knowledge) film growth provides many potential uses which are presented now.

4.1 ULTRA-THIN FILMS. — The low surface diffusion of deposited clusters implies no dramatic coalescence of incident particles during the first stages of film growth. So, for metal/substrate systems presenting a high atomic diffusion surface coefficient, LECBD can be used to minimize the critical thickness (d_c) at which the film becomes continuous. For instance, we have shown that LECBD Sb films have a critical thickness d_c ten times smaller than MBD Sb films deposited under the same conditions (vacuum, substrate temperature, deposition rate, ...). Electrical measurements show that d_c decreases from 37 nm for MBD to 2.2 nm for LECBD films. This is illustrated in figure 5 which shows the evolution of the Sb film conduction current *versus* its equivalent thickness (d). In both cases (MBD and LECBD), the low current value observed at very low thicknesses shows that Sb tends to form isolated islands. Then these Sb islands grow for increasing d and the electric current can flow from one electrode to the other when a conducting path appears. For LECBD deposits, the growth of isolated islands is much less significant than for MBD. This leads to a lower d_c value for LECBD films [5].

The random packing of incident clusters allows the formation of ultrathin films at room temperature. In addition, this film growth mode suggests that ultra-thin metallic films can be synthesized on any support since the diffusion of supported aggregates can be reduced by increasing the size of free clusters. This would improve the reproducibility of thin film deposition.

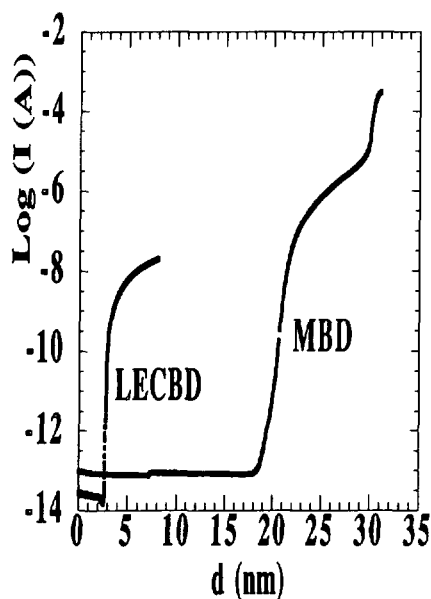


Fig. 5. — Plot of the observed current I versus film thickness during cluster deposition of Sb_{1850} (LECBD) and Sb_4 (MBD). The difference in nucleation and growth processes is evidenced by the shift of the electrical percolation threshold d_c toward low thickness for LECBD deposit ($d_c = 37$ nm for MBD and 2.2 nm for LECBD Sb deposits).

4.2 EXPERIMENTAL MODEL SYSTEM.

4.2.1 Cluster-cluster aggregation. — We have seen in the paragraph devoted to LECBD film growth that, roughly, the film grows by coating of the substrate with incident clusters. The

lower the substrate temperature, the better the approximation. This allows us to interpret the film growth in terms of percolation theory. Two main models (diffusion limited aggregation (DLA) [20] and cluster-cluster aggregation (CCA) [21]) have been developed by theoreticians to interpret experiments where dynamical effects are important.

To achieve these models by LECBD we deposit clusters on a substrate held at low temperature (180 K). At this temperature, the particle distribution is close to the distribution of the free clusters, with a small shift toward larger sizes probably due to the geometric overlap of first neighbors (direct capture) occurring during deposition. An interesting phenomenon arises when the temperature increases : supported clusters diffuse on the surface and the deposit morphology is modified as shown in figure 6. These experimental images correspond well to those in the CCA or DLA models. Why do we get such aggregates ? As isolated clusters



Fig. 6. — Effect of warming up (rate of 1 K/mn) from 180 K (substrate temperature during deposition) to room temperature on a 0.02 nm thick antimony deposit, obtained with a Sb_{1200} cluster beam.

diffuse at high temperatures, we assume that they just stick together when they touch (without merging in a single particle) as in the CCA model. This simple picture has to be refined because of the presence of surface defects which certainly act as nucleation centers, maybe generating some bigger aggregates similar to the DLA ones.

We see that cluster deposition, contrary to atomic or molecular deposition, permits an experimental comparison with several 2D theoretical models (percolation, cluster-cluster aggregation). This will be fruitful for theoreticians who might also be tempted to try to reproduce our experimental results by improving their simulations. On the other hand, comparison of our experiments with many theoretical models (think of the fractal dimension) will allow a better understanding of the LECBD film growth mechanisms.

4.2.2 Nucleation transient regime study : a challenge for theoreticians. — Film deposition usually proceeds through nucleation and growth stages. Two theoretical approaches (chemical or diffusion governed models) developed during the past two decades [22-24] well describe the abundant experimental results given by TEM studies [25-29]. For these models, the main nucleation parameters are the residence time of the adatom, the binding nucleation energy (that gives the critical cluster size), the surface diffusion and the substrate nature. Many regimes of condensation are exhibited : 2D or 3D growth, complete or incomplete condensation regime. As the nucleation of stable clusters occurs when an adatom diffuses to join a critical cluster, one of the main parameters is the capture time (τ_c) corresponding roughly to the time where adatom population decreases by stable cluster capture. This time τ_c increases as the adatom diffusion decreases. τ_c is too low to be measured in classical experimental conditions.

For LECBD films, the classical theory could be adapted to describe the free cluster nucleation. In this case, the order of magnitude of the classical parameters is changed. The main difference is :

- reevaporation is negligible ;
- all the « *adclusters* » are stable clusters ;
- the diffusion coefficient is very low ;
- τ_c is high ;
- in addition, the *adcluster* population is easily observable by TEM.

Finally, the film is formed by *adclusters* and some bigger clusters corresponding to the accretion of *adclusters*. Using classical nucleation predictions, one observes this behaviour in the transient regime ($t < \tau_c$). Work is in progress to study this particular regime [30].

4.3 NEW STRUCTURAL PROPERTIES OF LECBD FILMS.

4.3.1 New structural properties : is it realistic ? — In this section we summarize the basic ideas which may drive the search of new properties of films grown by cluster deposition. We present the frame in which LECBD films with unusual electronic properties are expected. First, the incident free clusters have to exhibit « quantum size effects » (so-called « molecular effects »). Then, these clusters have to survive on the substrate without shape and internal structure change. These problems are discussed now.

The study of the transition between atom and bulk is already fully developed. For metallic clusters, some properties such as magic numbers, potential ionization oscillations *versus* cluster size, critical size corresponding to an insulator-metal transition are extensively studied by spectroscopic methods [31, 32]. The critical cluster size to observe quantum size effects in free clusters is an important parameter. For alkaline metals, all experiments seem to corroborate that a cluster size of 1-2 nm is a « *piece of metal* » regarding « collective properties » (for example plasma oscillations [33]). Here, an individual atom has one electron in the s shell but as $\langle N \rangle$ increases, the s shells merge into one half-filled conduction band.

Except the problem of « shells » [34] and « supershells » [35] due to bunching of levels, these clusters gradually assume bulk-like properties (metallic behavior), which are reached for roughly one hundred atoms.

In a more general way, the « quantum properties » are governed by the surface atoms. As $\langle N \rangle$ increases, the surface/bulk atom ratio $N_{\text{surf}}/N_{\text{bulk}}$ decreases and the probability to preserve the molecular character becomes lower. For example, a fcc cubo-octahedron with 1 529 atoms has a ratio $N_{\text{surf}}/N_{\text{bulk}} = 0.58$ [36]. So, only elements with « complex » electronic structure (for example a partial filled p-d or f band) are expected to exhibit some new properties.

For these « complex electronic elements » the problem is then to know whether the cluster film preserves the « memory » of the free cluster structure. The energy per atom $E/\langle N \rangle$ in the cluster increases as the cluster size decreases and so the comparison of $E/\langle N \rangle$ with ε (ε is the cluster binding energy : in the case of antimony, Sb cluster is considered as a packing of Sb_4 and ε is the energy to remove an Sb_4 entity from the cluster) is helpful to determine when clusters are expected to survive in the initial state. For $E/\langle N \rangle \geq \varepsilon$, fragmentation probability of the cluster is large (fragmentation or successive evaporation). For $E/\langle N \rangle \ll \varepsilon$ free clusters survive in the initial state. In the intermediate stage, the cluster survives with atomic rearrangements, local heating or melting and recrystallization. If the free cluster « quantum size » properties correspond to a metastable state, all the « new » properties are lost after recrystallization. The ideal solution is to deposit cold clusters without kinetic energy. In the « best » cluster sources (high supersaturation ratio with cold carrier gas), the vibrational cluster temperature is about a few hundred K with a kinetic energy corresponding to a velocity roughly equal to the carrier gas. $E/\langle N \rangle \varepsilon$ data for antimony clusters (Fig. 7) show that the LECBD technique reaches a regime of soft landing ($E/\langle N \rangle \ll \varepsilon$) in a large range of cluster sizes.

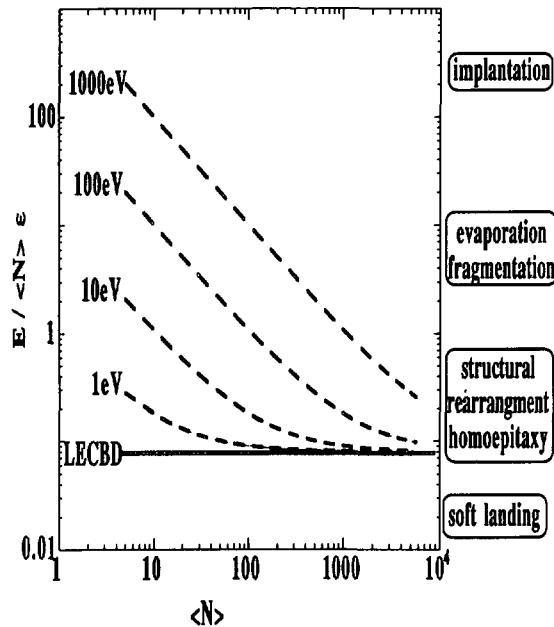


Fig. 7. — Evolution of $E/(\langle N \rangle \varepsilon)$ versus $\langle N \rangle$ where E , $\langle N \rangle$ and ε are respectively the total cluster energy, the mean atom number per cluster and the Sb binding energy. The physical phenomena corresponding to particular $E/(\langle N \rangle \varepsilon)$ range are deduced from Müller assumptions [42]. This estimation is rough because we assume that the energy is randomly distributed among internal modes.

Lastly, the small supported clusters surviving with their initial structure (presenting quantum size effects) have also to avoid coalescence. The surface diffusion of small clusters (size lower than 1-2 nm) allows large island formation by nucleation and coalescence effects. So, we expect to obtain thick films by stacking of clusters only for large incident clusters (LECBD films) or for very low substrate temperatures (MBD films).

So, two conditions have to be satisfied to synthesize new structural properties of cluster films :

- cluster size small enough to observe quantum size effects
- cluster size big enough to preserve the memory of free cluster (low surface diffusion regime).

It is true that these two conditions seem to be satisfied in the LECBD technique according to the experimental results presented below.

4.3.2 Two examples. — The main result obtained is that LECBD allows the preparation of *continuous* and *amorphous* antimony films stable at room temperature, whereas such films have never been obtained by MBD at room temperature [6]. Continuous amorphous Sb films obtained by other conventional methods are unstable at RT. For these films the amorphous-crystal transformation occurs at about $T_c = 250$ K. LECBD films are amorphous and crystallize at 323 K. TEM observations show that each amorphous domain crystallizes individually in the normal rhomboedral Sb structure without any shape or grain size modification [6]. In addition, this LECBD amorphous antimony phase presents a particular electronic structure as shown by electron transport studies (see Sect. 5).

Another experimental result can be extracted from our studies on the lanthanides. The lanthanides exhibit many crystallographic structures. Samarium, like all the lanthanides (except lanthanum, ytterbium and lutetium), shows a valence change from the $4f^N (5d^0 6s^2)$ state to the trivalent $4f^{N-1} (5d^1 6s^2)$ state [37]. In addition, Sm clusters present a mixed state of divalent and trivalent states. The f electron is highly localized and brings a weak contribution to bonding. Both configurations are nearly degenerate. The trivalent state requires a large coordination number to promote f orbital overlap. Theoretical calculations and experimental results show that the surface atoms are in a divalent state while atoms of the particle core have the trivalent configuration [38, 39]. Calculations using one-electron models show a strong correlation between the electronic and the crystallographic structure (37). Thin samarium LECBD films (4 nm Sm supported clusters in our experiment) exhibits an fcc structure while the common is Sm-type. This new structure corresponds to a commensurate phase that accommodates the large lattice parameter of divalent surface atoms (a small lattice will promote the overlap and the divalent-trivalent transition) and trivalent core atoms of the supported particles [40]. This new phase is a consequence of « quantum size effects ». Such effects are easily observed in samarium (as a consequence of Hund's rule) because the f band is practically half filled.

4.4 NANO-SPONGE. — In addition to the first asset of the LECBD technique, which is the direct control and the low value of grain size of metallic films, the high roughness of LECBD will play a crucial role in the improvement of chemical reactivity of surfaces. A typical use of the roughness profile properties and the small grain size of the LECBD films is the giant surface/volume ratio. This « nano-sponge » behavior is clearly observed by electrical measurements for Bi LECBD films. To compare the LECBD and MBD film reactivity with oxygen, we have measured, after deposition, the resistance evolution of these samples under 600 Pa of O_2 (Fig. 8). Notwithstanding the higher resistance of the LECBD Bi deposits, LECBD films are much more sensitive to air exposure than MBD ones : after introduction of oxygen in the deposition chamber, the oxidation of the LECBD film causes a large increase of the electrical resistance. In comparison, the electrical resistance of MBD films remains

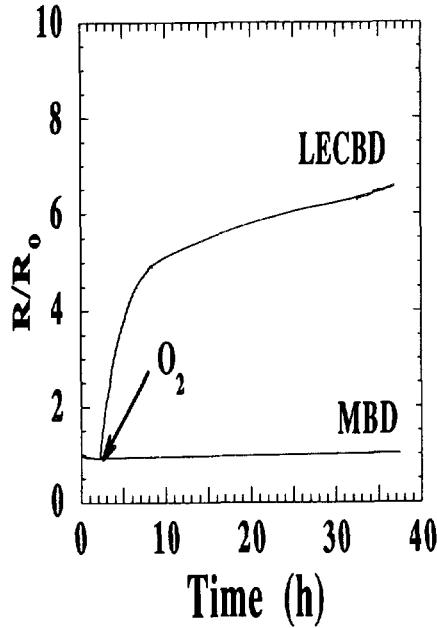


Fig. 8. — Relative resistance of MBD (curve a) and LECBD (curve b) as function of time during O_2 exposure ($P_{O_2} = 600$ Pa). In both cases the equivalent film thickness is 36 nm.

unchanged. The morphology of deposits and especially the higher roughness and the low grain size of LECBD Bi films explain such a behavior [41].

The general behavior of the film microstructure agrees with the molecular dynamics simulation of Müller [42]. Taking into account the mean velocity of the free clusters and the internal thermal energy, the mean energy per atom in the cluster $E/\langle N \rangle$ does not exceed 0.1ε (for example $\varepsilon = 2.75$ eV for antimony bulk phase). Müller's simulations give a random stacking of small free incident particles on the substrate, and our experimental results (TEM, diffraction pattern and Raman analysis) corroborate the disordered stacking of LECBD films that can be considered as perfectly rough films.

4.5 ELECTRON LOCALIZATION EFFECTS IN LECBD FILMS. — In crystalline solids localized states are introduced by chemical impurities or by stratification of the electronic states in a very thin film (2D), thin wire (1D) or nanograin (0D). On the other hand, in an amorphous solid, the disorder induces localized states. The most common localized-extended state transition (usually called insulator-metal transition) corresponds to the models of Mott [43] and Anderson [44]. In Mott's model, the electron-electron correlation energy is the origin of the localized states. For conventional tetrahedrally bonded semiconductors, the localized states near the Fermi level increases with the material disorder. Assuming Mott's transport model, the dc conductivity σ_{dc} of a semiconductor is roughly described by two terms :

$$\sigma_{dc} = \sigma_{h0} e^{-(T_0/T)^{1/n}} + \sigma_a e^{-E_a/k_B T}$$

where T_0 is related to the density of localized states at the Fermi level, σ_{h0} , σ_a are prefactors, n an integer, E_a an activation energy and k_B Boltzmann's constant. The first term corresponds to the mechanism of variable range hopping. For thick films $n = 4$. For thin films (thickness lower than the average hopping distance of the electrons d_a (10-20 nm [45]), $n = 3$. The second

term corresponds to the activated conduction roughly described by direct or indirect transition between the states near the Fermi level and the bottom of the conduction band. This contribution becomes larger at high temperatures.

In Anderson's model, localization is not due to electron-electron correlations but to the random fluctuation of the potential induced by the topological disorder in amorphous materials. Roughly localization takes place when the width of the potential fluctuation exceeds the overlap bandwidth.

Antimony is one of the best candidates to study disorder effects. Amorphous Sb is a semiconductor quite similar to tetrahedrally bonded semiconductors such as a-Ge [46]. The crystallized phase is a semi-metal having low but degenerate carrier concentrations with threefold coordination (0.16 eV band overlap). The electronic properties of Sb strongly depend on the local atomic structure which leads to a strong dependence between transport properties such as dc conductivity and localization effects induced by disorder.

4.5.1 Pure material without localization effect. — The dc conductivity of pure crystallized bulk antimony is about $\sigma = 2.56 \times 10^4 \Omega^{-1} \text{cm}^{-1}$ at 273 K [47]. MBD films (formed by hemispherical crystallized grains of 100 nm diameter) give a lower conductivity (typically $\sigma \approx 10^3 \Omega^{-1} \text{cm}^{-1}$). Two factors explain this lower value : the polycrystalline phase and the low film thickness, as shown by Damodara *et al.* [48]. The conductivity is dependent on temperature (with a positive TCR (temperature coefficient of resistance)) and proportional to the thickness of the film. Transport properties are typically the semi metal ones.

4.5.2 « Weak » localization : LECBD crystallized film. — LECBD crystallized films with a macroscopic disorder of grain stacking (see Fig. 3) present unique characteristics to conduct « electron localization effects » studies. Because of the very small grain size and the high disorder between the crystallized clusters, « localization » is expected to give anomalies in transport effects in these nanocrystallized materials. The LECBD technique can give thick Sb films (more than 100 nm) with a 5 nm grain size. Since the antimony grains are individually crystallized with strong and random mismatch between them, potential barriers between the particles are involved and the Anderson model can describe the electronic conduction of LECBD films. It should be observed that the random barriers correlated to grain boundaries exhibit two kinds of random character : random periodicity in real space induced by random stacking and random depth of barrier potential induced by random surface contact between grains. The low conductivity of LECBD crystallized Sb films ($330 \Omega^{-1} \text{cm}^{-1}$ compared to $2.56 \times 10^4 \Omega^{-1} \text{cm}^{-1}$ in bulk) is noteworthy. Neglecting the effect of cluster surface oxidation on the measurement of σ ⁽¹⁾, the low conductivity of LECBD crystallized Sb films could be explained by localization effects. In addition, the dependence of σ on T shows a negative TCR (Fig. 9) which may have two likely origins :

1) In semi-metals, the de Broglie electron wavelength (approximately 6 nm in pure antimony [49]) corresponds roughly to the film grain size and so quantum size effects can occur. A similar behavior (negative TCR) is observed by many authors in ultra-thin films of semi metals [50]. The valence band and the conduction band split up into discrete layers

(1) The profile XPS analysis of LECBD films shows two peaks attributed to metallic Sb and to Sb-O bondings. Previous TEM studies show [58] that the deposited clusters may be formed by a pure metallic core surrounded by an oxide shell. The presence of an antimony oxide on the cluster surface does not modify the electronic structure of the metallic core but it plays a crucial role in the film morphology. The stability of nanocluster packing may be due to the surface oxide presence which induces an energy barrier at the interface, promoting the electron localization. This barrier is evidenced by the high activation energy during the amorphous-crystalline phase transition of LECBD films [6].

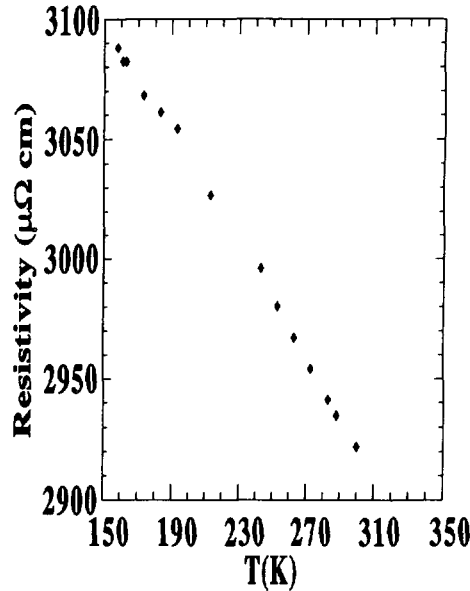


Fig. 9. — Evolution of the electrical resistivity ρ of a 13.5 nm-thick antimony LECBD film. A Sb_{2000} cluster beam has been used to synthesize this film. After deposition the deposit has been crystallized (irreversible process) by thermal annealing at 350 K. The $\rho(T)$ curve presented here is recorded after this crystallization. $\rho(T)$ dependence shows a negative TCR of Sb crystallized LECBD films.

inducing the disappearance of the band overlap : a semi-metal to insulator transition occurs [51]. The critical size N_c (corresponding to d_c mean diameter) corresponding to the semi-metal-semiconductor transition is given by :

$$d_c < (\hbar^2 \pi^2 / (2(m_e^* + m_h^*) \Delta))^{1/2}$$

where m_e^* , m_h^* are respectively the electron and hole effective masses and Δ the bulk band overlap [51]. Using the published data ($m_e^* = 0.09 m_0$, $m_h^* = 0.1 m_0$, $\Delta = 0.16$ eV [52]), the critical size is calculated to be about 4 nm. This value is in the same range as the mean cluster size and so localization effects can be observed.

2) Nevertheless, the discrete band effect cannot be taken into account in our temperature range (100-350 K). In this temperature range the thermal energy becomes of the same order of magnitude as the pseudo-gap between two discrete levels, and the semi-conductor behavior is expected to be destroyed. For this reason, a more likely origin of the localization effects can be proposed. The localization corresponding to the random stacking gives a negative TCR as shown by Dynes *et al.* [53]. They have shown that the LuRh_4B_4 film resistivity change from positive to negative TCR as the disorder increases (disorder induced by α -particle irradiation). Buckel and Hilsch [54] have also observed a similar behavior in disordered bismuth films, the transport properties of which are expected to be close to the Sb ones.

To sum up the original transport properties of LECBD Sb films, we show now that each grain can be considered as a 0D conductor (nanograin conductor). Using the quasi-free electron formalism, it is possible to estimate the electrical resistivity of LECBD Sb films. Because of the low effective mass of the carriers in antimony, the carriers move inside the cluster without collisions creating a degenerated Fermi gas. So, the transport properties can be understood

roughly in the free electron formalism and the electrical resistivity is written in the general form :

$$\rho = \frac{3}{e^2 \lambda V_F N(E_F)}$$

where λ is the mean free path, e the electron charge, V_F the Fermi velocity (10^8 cm s^{-1}) and $N(E_F)$ the density of states at the Fermi energy (about $5 \times 10^{19} \text{ eV}^{-1} \text{ cm}^{-3}$ at $E_F = 0.33 \text{ eV}$ in the bulk phase) [55]. The mean free path is given roughly by the cluster size and the calculated value of ρ ($7.5 \times 10^{-3} \text{ } \Omega\text{cm}$) is in the range of our experimental data ($3 \times 10^{-3} \text{ } \Omega\text{cm}$). This shows that the resistivity of crystallized LECBD thin film is entirely governed by the cluster size.

This suggests an interesting correlation between LECBD deposits and quasicrystalline structure in which the pseudo-gap appears as a consequence of localization effects. For the quasicrystalline structure, the pseudo-gap appears as a result of the Fermi surface-Brillouin zone boundary interaction. For LECBD deposits, assuming that a cluster is a Wigner-Seitz cell, a pseudo-Brillouin zone can be calculated in the Fourier space (« artist view »). Roughly, for a 5 nm cluster size, one obtains a quasi reciprocal lattice vector $K = 0.12 \text{ } \text{Å}^{-1}$ ($K \approx 2 \pi/d$). It is important to note here that this value corresponds roughly to $2 k_F$ ($0.18 \text{ } \text{Å}^{-1}$ for antimony) which is the appropriate condition for creating gaps around the Fermi energy (Bragg-Laue reflexion $k_F = K/2$). This condition exists in some quasicrystalline structures and this is the basis of the analogy between the « Hume-Rothery » alloys and quasicrystalline structures [56]. The similitude between quasicrystalline structure and LECBD films is evidenced by the common value of the TCR coefficient of LECBD film and Al-Li-Cu I-phase alloy. In the range 150 K-350 K, the TCR value [55] is about $4 \times 10^{-4} \text{ K}^{-1}$ in both cases.

Despite the apparent difference between quasicrystalline structure (no medium range order, and long range order) and LECBD deposits (medium range order but no long range order), the correlation between quasi-crystals and LECBD films seems to be valid for transport properties.

4.5.3 High localization : LECBD amorphous phase. — Usually, dc conductivity measurements of Sb films obtained by conventional deposition techniques are very sensitive to thermal annealing. On the other hand, LECBD films are very stable above the crystallization temperature and successive thermal annealing of the Sb films does not induce appreciable conductance variations [6]. In spite of the large temperature range studied, variable range hopping is the predominant mechanism. The critical T_c corresponding to the conduction mechanism transition (variable range hopping \rightarrow activated conduction) increases strongly (160 K (conventional films) \rightarrow 260 K (LECBD)). This T_c increase can be understood in terms of disorder increase. This shows two disorder levels : the conventional disorder inside the grain (which promotes the variable range hopping) and a disorder related to the stacking of grains of different sizes (which promotes Anderson model localization). Figure 10 gives the conductance scale for Sb films obtained by various methods. The large range of conductance values (10^6) is the signature of the decrease of disorder from the LECBD amorphous films to the crystalline phase.

The LECBD technique allows the synthesis of thin films for which the exploration of the whole scale of electron localization effects can be possible. Figure 11 summarizes the basic mechanisms of transport properties of LECBD films. For an ideal LECBD film (a long range ordered packing of single size crystalline clusters), electrons are in a Kronig-Penney potential (Fig. 11a). For experimental LECBD crystallized films, the potential of Anderson has to be considered (a further localization) (Fig. 11b). In amorphous LECBD films, the electron-

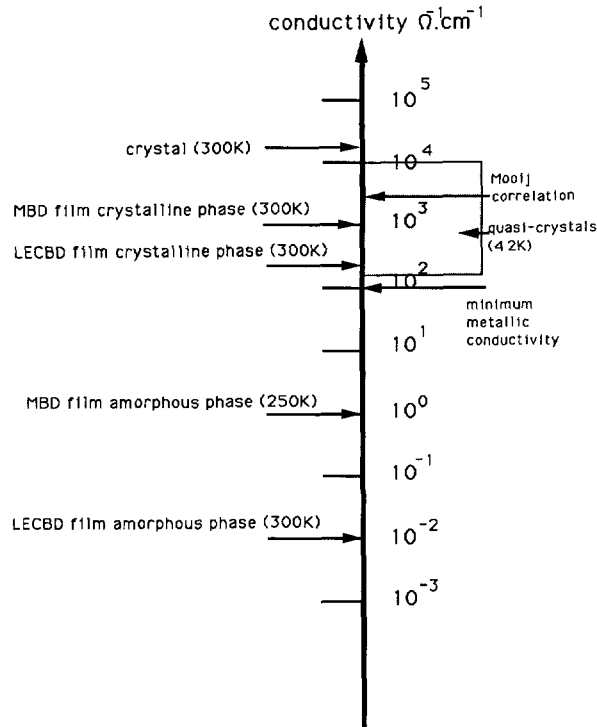


Fig. 10. — Conductance values of antimony deposits obtained by various deposition methods. The Mott criterion of the insulator-metal transition predicts $\sigma = 10^2 \Omega^{-1} \text{cm}^{-1}$ [43]. The order of magnitude of σ is given by the Mooij correlation ($\sigma = 7 \times 10^3 \Omega^{-1} \text{cm}^{-1}$) [57]. The range of σ for quasi crystalline materials is also reported [55].

electron interaction due to the disorder induced by the amorphous phase leads to the Mott localization.

Experimental results for antimony show that these cases can now be studied :

1) before crystallization (deposition at room temperature), the deposits are amorphous and strong localization effects are evidenced (Fig. 11c) and

2) after crystallization, the deposits are formed with small crystalline aggregates presenting similar effects than « weak localization ones » (Fig. 11b).

While the size of supported aggregates obtained by MBD is larger than the electron elastic mean free path, the LECBD technique allows now to study these localization effects.

5. Conclusion.

The physical and chemical properties of films prepared by LECBD show promising technological and theoretical applications of this deposition technique. LECBD film growth can be described as a random stacking of nano-clusters leading the formation of continuous ultrathin films or deposits with a giant surface/volume ratio. In addition, the original electronic structure of free clusters due to quantum size effects can be preserved after deposition on the substrate. From these results, many research fields can be explored now. Since new phases have been synthesized with this deposition technique (amorphous antimony thick films stable at room temperature, fcc samarium deposits), a wide variety of new materials could be

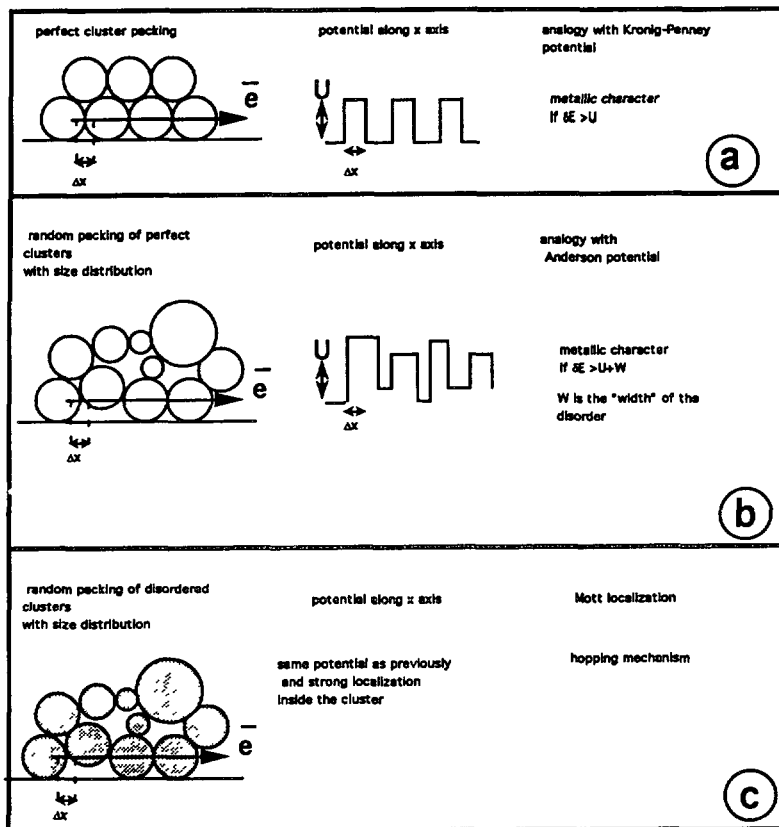


Fig. 11. — a) Basic mechanisms describing transport properties of ideal LECBD films : a long range ordered packing of single size crystalline clusters ; b) experimental crystallized LECBD films ; c) experimental amorphous LECBD films. δE represents the free electron energy.

achieved by this deposition technique. In the case of semi-metals for which the Fermi surface is very small and of the same order as the dimension of the pseudo Brillouin zone, new transport properties are expected. Since the cluster size controls directly the pseudo Brillouin zone, it seems possible now to explore all values of the quasi reciprocal lattice vector K for a given material.

Reference

- [1] AVERBACK R. S., BERNHOLC J., NELSON D. L., « Clusters and Cluster-Assembled materials » Mat. Res. Soc. Symp. Proc., vol. 206, R. S. Averback, J. Bernholc, D. L. Nelson Eds. (Pittsburgh, Pennsylvania Boston, 1990).
- [2] YAMADA I., *Phys. Scr.* T 35 (1991) 245.
- [3] YAMADA I., *Nucl. Instrum. Methodes* B 55 (1991) 544.
- [4] YAMADA I., *Appl. Surf. Sci.* 43 (1989) 23.
- [5] MÉLINON P., JENSEN P., HU J. X., HOAREAU A., CABAUD B., TREILLEUX M., GUILLOT D., *Phys Rev. B* 44 (22) (1991) 12562.
- [6] JENSEN P., MÉLINON P., TREILLEUX M., HOAREAU A., HU J. X., CABAUD B., *Appl. Phys. Lett.* 59 (12) (1991) 1421.

- [7] FUCHS G., MÉLINON P., TREILLEUX M., LE BRUSQ J., *J. Phys. D* **26** (1993) 143.
- [8] FUCHS G., MÉLINON P., TREILLEUX M., *J. Phys. I France* **2** (1992) 1263.
- [9] SATTLER K., MUHLBACH J., RECKNAGEL E., *Phys. Rev. Lett.* **45** (1980) 821.
- [10] MÉLINON P., Ph. D. Thesis, University of Lyon (France, 1986).
- [11] RAYANE D., MÉLINON P., TRIBOLLET B., CABAUD B., HOAREAU A., BROYER M., *J. Chem. Phys.* **91** (1989) 3100.
- [12] BROYER M., CABAUD B., MÉLINON P., RAYANE D., TRIBOLLET B., *Mol. Phys.* **62** (1987) 559.
- [13] FUCHS G., MÉLINON P., SANTOS AIRES F., TREILLEUX M., CABAUD B., HOAREAU A., *Phys. Rev. B* **44** (8) (1991) 3926.
- [14] METZGER R. A., ALLEN F. G., *Surf. Sci.* **137** (1984) 397.
- [15] STREIT D. C., METZGER R. A., ALLEN F. G., *Appl. Phys. Lett.* **44** (1984) 234.
- [16] SIUGURA H., *J. Appl. Phys.* **51** (1980) 2630.
- [17] FUCHS G., TREILLEUX M., SANTOS AIRES F., CABAUD B., MÉLINON P., HOAREAU A., *Phys. Rev. B* **40** (10) (1989) 6128.
- [18] JENSEN P., MÉLINON P., HOAREAU A., HU J. X., CABAUD B., TREILLEUX M., BERNSTEIN E., GUILLOT D., *Physica A* **185** (1992) 104.
- [19] BERTHIER S., Private communication.
- [20] WITTEN T., SANDER L., *Phys. Rev. Lett.* **47** (1981) 1400.
- [21] KOLB M., BOTET R., JULLIEN R., *Phys. Rev. Lett.* **51** (1983) 1123.
- [22] VENABLES J. A., SPILLER G. D. T., HANBUCKEN M., *Rep. Prog. Phys.* **47** (1984) 399.
- [23] ZINSMEISTER G., *Thin Solid Films* **7** (1971) 51.
- [24] STOWELL M. J., HUTCHINSON T. E., *Thin Solid Films* **8** (1971) 411.
- [25] REICHEL K., *Vacuum* **38** (12) (1988) 1083.
- [26] VELFE H. D., STENZEL H., KROHN M. D., *Thin Solid Films* **98** (1982) 115.
- [27] USHER B. F., ROBINS J. L., *Thin Solid Films* **90** (1982) 15.
- [28] HENRY C., CHAPON C., MUTAFSCHIEV B., *Thin Solid Films* **L1** (1976) 33.
- [29] VAN HARDEVELD R., HARTOG F., *Surf. Sci.* **15** (1969) 189.
- [30] HU J. X., Ph. D. Thesis, University of Lyon (1992).
- [31] SCHUMACHER E., *Chimia* **42** (1988) 357.
- [32] « Small Particles and Inorganic clusters », Proc. ISSPIC 5 (Konstanz, 1990) O. Echt, E. Recknagel Eds., *Z. Phys. D* **19-20** (1991).
- [33] SELBY K., KRESIN V., MASUI J., VOLLMER M., DE HEER W. A., KNIGHT W. D., *Phys. Rev. B* **40** (1989) 5417.
- [34] KNIGHT W. D., CLEMENGER K., DE HEER W. A., SAUNDERS W. A., CHOU M. Y., COHEN M. L., *Phys. Rev. Lett.* **52** (1984) 2141.
- [35] NISHIOKA H., Atoms, Molecules and Clusters, *Z. Phys. D* **19** (1991) 19.
- [36] VAN HARDEVELD R., HARTOG F., *Surf. Sci.* **15** (1969) 189.
- [37] SKRIVER H. L., Systematics and the Properties of the lanthanides, NATO ASI Series, Serie C, Mathematical and Physical Sciences, D. Reidel **109** (Publishing Company, Eds., 1982).
- [38] FALDT Å., MYERS H. P., *Phys. Rev. B* **52** (15) (1984) 1315.
- [39] WERTEIM G. K., CRECELIUS G., **40** (12) (1978) 813.
- [40] MÉLINON P., FUCHS G., TREILLEUX M., *J. Phys. I France* **2** (1992) 1263.
- [41] FUCHS G., MONTANDON C., TREILLEUX M., CABAUD B., MÉLINON P., HOAREAU A., *J. Phys. D*, in press (1993).
- [42] MULLER K. H., *J. Appl. Phys.* **61** (7) (1987) 2516.
- [43] MOTT N. F., « Metal-insulator transitions » (Taylor and Francis, London, 1974).
- [44] ANDERSON P. W., *Phys. Rev.* **109** (1958) 1492.
- [45] MACKINTOSH A. J., PHILLIPS R. T., YOFFE A. D., *Physica B + C* **117, 118** (2) (1983) 1001.
- [46] HAUSER J. J., *Phys. Rev. B* **11** (2) (1975) 738 ; *Phys. Rev. B* **9** (6) (1974) 2623.
- [47] ASHCROFT N. W., MERMIN N. D., « Solid State Physics », D. Garboe Crane, Ed., ISBN 0-03-049346-3 (1976).
- [48] DAMORA V., SOUNDARAJAN N., *J. Mater. Sci.* **24** (1989) 4315.
- [49] « Physics of thin films », Advances in Research and Development, G. Hass, R. E. Thun, Eds., Vol. 6 (Academic press, New York, 1971) pp. 81-149.

- [50] A negative TCR has been observed in thick bismuth films in which the quantum size effects should not appear. If the mean free path (mfp) is lower than the sample dimension, the reduction of carrier density as function of the temperature is not counterbalanced from the mfp increase. This effect is particular to bismuth with an high value of mfp ($> 1\ 000$ nm at 300 K).
- [51] SANDOMIRSKII V. B., *Sov. Phys. JETP* **25** (1967) 101.
- [52] VOLKEIN F., *Thin Solid Films* **191** (1990) 1.
- [53] DYNES R. C., ROWELL J. M., SCHMIDT P. H., In Ternary Superconductors, G. K. Shenoy, B. D. Dunlap, F. Y. Fradin, Eds. (North-Holland, Amsterdam, 1981).
- [54] BUCKEL W., HILSCH R., *Z. Phys.* **138** (1954) 109.
- [55] KIMURA K., TAKEUCHI S., « Quasicrystals : the state of the Arts », D. P. Vincenzo, P. Steinhardt, Eds. (Word Scientific Publishing Co., 1991) pp. 313-342.
- [56] FRIEDEL J., DENOYER F., *C. R. Acad. Sci. Paris* **305** (1987) 171.
- [57] MOOU J. H., *Phys. Status Solidi A* **17** (1973) 521.
- [58] FUCHS G., TREILLEUX M., SANTOS AIRES F., CABAUD B., MÉLINON P., HOAREAU A., *Philos Mag.* **63** (3) (1991) 715.